PAPER

Check for updates

Enhanced water permeability across a physiological droplet interface bilayer doped with fullerenes†

Jean-Baptiste Fleury ID *

We measure the water permeability across a physiological lipid bilayer produced by the droplet interface bilayer (DiB) technique. This lipid bilayer can be considered as physiologically relevant because it presents a lipidic composition close to human cell membranes. The measured water permeability coefficients across this lipid bilayer are reported as a function of the cholesterol concentration. It is found that the water permeability coefficients decreased with increasing cholesterol concentration, in agreement with the existing literature. And, consistently, the extracted corresponding activation energies increase with increasing cholesterol concentration in the lipid bilayer. Hence having demonstrated the robustness of the experimental system, we extend this study by exploring the influence of fullerenes on the water permeability of a physiological lipid bilayer. Interestingly, we observe a significant increase of the measured water permeability coefficients across this lipid bilayer for large fullerenes concentration. This enhanced permeability might be related to the conductive properties of fullerenes.

1 Introduction

Fullerene is a small, hollow and hydrophobic carbon nanoparticle that has attracted attention for its potential in biomedical applications.[1] Fullerene derivatives are being investigated as vectors for drug delivery, diagnostic contrast agents, antioxidants, or as antiviral agents against human immunodeficiency virus (HIV-1).[2–4] This versatility can be explained by the fact that fullerene could be easily functionalized with many bioactive compounds like peptides or saccharides.[1] Additionally fullerene exhibits interesting electronic and optical properties, as an example, common fullerene derivatives (fullerides) are members of a larger family of organic conductors.[5] And fullerene-derived polymeric materials are key components in photovoltaic cells.[6] Despite these advantages, fullerenes and their derivatives have raised questions and concerns about their nanotoxicity and environmental impact.[7–9] Recent reviews seem to indicate that fullerene is not toxic, but the toxicity of fullerene-derivatives must be determined before use *via* clinical studies.[8,9]

One challenge that limits the usage of fullerene for biomedical applications is its dissolution.[10] Fullerene is substantially insoluble in polar solvents, such as water.[10] It is almost insoluble in apolar solvents, *i.e.* its solubility in alkanes is rather low (only 25 μg mL^{-1} in octane). The few good solvents for fullerene are toxic; like toluene and carbon disulfide.[10,11] To

overcome this difficulty and possibly deliver fullerene into cells, lipid vesicles have been employed as a carrier to dissolve and carry the fullerene in an aqueous phase.[11,12] Studies have reported the successful incorporation of a large concentration of fullerenes (up to 30%) into stable liposomes.[13] However, the physical properties of such entities have been barely studied.[11,13]

Lipid bilayer membranes are important as fundamental structures in biology that are present in all living cell membranes.[14] They provide characteristic water-permeability, stability, and mechanical properties to the cell membrane. In particular, perturbation of membrane water-permeation causes osmolality changes in body fluid that may lead to health issues.[15] And as fullerene could be delivered to cell membranes *via* liposomes, it is relevant to investigate how these fullerene molecules are affecting the water permeation of cell membranes.[11] In particular, investigations into membrane permeation of water of these liposomes seems to have been limited to theoretical investigations.[11,12,16] It is also interesting to note that this type of question has not been considered during the toxicological studies mentioned previously.[8,9]

In this manuscript, we measure the water permeation across a lipid bilayer doped with fullerenes. We produce a free-standing lipid bilayer using the droplet interface bilayer (DiB) technique.[17] This method consists of dispersing two spherical water droplets in an oily phase that contains phospholipids. Thus the two water–oil droplets interfaces are rapidly decorated by a phospholipid monolayer. Then the two monolayers are brought into contact manually to spontaneously form a free-standing lipid bilayer.[17] Then applying an osmolality difference between the two droplets, we could measure the exchange of water and any volume change in these droplets using optical

Experimental Physics and Center for Biophysics, Saarland University, D-66123 Saarbruecken, Germany. E-mail: jean-baptiste.fleury@physik.uni-saarland.de; Tel: +49 681 302 70121

† Electronic supplementary information (ESI) available. See DOI: 10.1039/d0ra01413c

microscopy. Thus, after analysis of these dynamical phenomena, we could extract the water permeability constant and its energy activation barrier *via* simple physical principles. These measurements are then performed as a function of fullerene concentration inside the lipid bilayer.

2 Materials and methods

2.1 Materials

Squalene oil was purchased from Sigma-Aldrich. DOPC (1,2-dioleoyl-*sn*-glycero-3-phosphocholine), DOPE (1,2-dioleoyl-*sn*-glycero-3-phosphoethanolamine), DOPS (1,2-dioleoyl-*sn*-glycero-3-phospho-L-serine (sodium salt)), cholesterol and fluorescent DOPE-rhodamine were all purchased from Avanti Polar Lipids. Fullerene-C60 (CAS 379646), and fullerene-C70 (CAS 482994), were purchased from Sigma-Aldrich. A glass container was purchased from VWR and coated with OTS (trichloro(octadecyl)silane, Sigma-Aldrich) to modify the hydrophobicity of the glass surface and avoid droplet spreading on its surface. Glass-OTS coating was performed *via* standard protocols. Ultra-pure water was obtained using a millipore purification system (Merck).

2.2 Lipid bilayer formation with the DiB method

Lipids are dissolved in squalene oil at the molar ratio mentioned in the following text and with a total mass concentration of 5 mg mL^{-1}. The lipids are left for 24 h at 50 °C under magnetic stirring. Then fullerene could be dissolved into this oil–lipid mixture. The OTS-coated glass container, which has a cylinder shape that is 1 cm in height and a diameter of 7 cm, is filled with the oil–lipid mixture. This device is placed on a home-made heat controller and covered by a micro-machined Teflon plate to keep the device thermostat at the desired temperature. The Teflon plate has a hole to allow optical investigation with a microscope (Leica Z16) connected to a PCO camera (PCO 1600). For formation and manipulation of an aqueous microdroplet, a micropipette with a desired tip, having a typical diameter in the range 1 mm was formed using a micropipette puller (Eppendor). By this method, two water droplets of nearly equal size are produce manually in this container, and left at rest for 30 min. They are brought, gently, into contact *via* a needle. After a few minutes, a bilayer appears spontaneously at the contact area between the droplets. The buffer composition of each droplet could be determined before droplet production. Thus an osmotic gradient could be achieved with two droplets having different concentrations of sodium chloride (NaCl, Sigma-Aldrich).

2.3 Surface tension and bilayer tension

Surface tensions of the various lipid monolayers at oil/water interfaces were measured with the pendant drop method using a commercial measurement device (OCA 20, DataPhysics Instruments GmbH, Filderstadt, Germany). An oil solution with a lipid total concentration of 5 mg mL^{-1} was produced by introducing a droplet from a steel needle into the surrounding oil phase. The shapes of all droplets were fitted with the Young–

Laplace equation to obtain their interfacial tension. After the initial formation of a droplet, the lipids adsorb on the interface, leading to a reduction in interfacial tension. This decrease was recorded over several minutes until a stable plateau was reached. Using these values of interfacial tension and the bilayer contact angle θ it is possible to calculate the tension of the lipid bilayer using the Young equation:[18]

$$\Gamma = 2\gamma \cos(\theta). \qquad (1)$$

The contact angle θ is obtained from optical micrographs of the formed lipid bilayer (Fig. 1A). The result is that the bilayer tension Γ is equal to ≈ 6.5 mN m^{-1} for a PC : PS : PE : Chol bilayer (70 : 10 : 20 and 40% cholesterol) in squalene oil (Fig. 1B).

2.4 Fluorescent measurements

The experimental setup used for these measurements is a standard epifluorescence setup. It consists of a computer controlled inverted microscope with a motorized focus system (Axio-Observer Z1, Zeiss), equipped with filter cubes containing
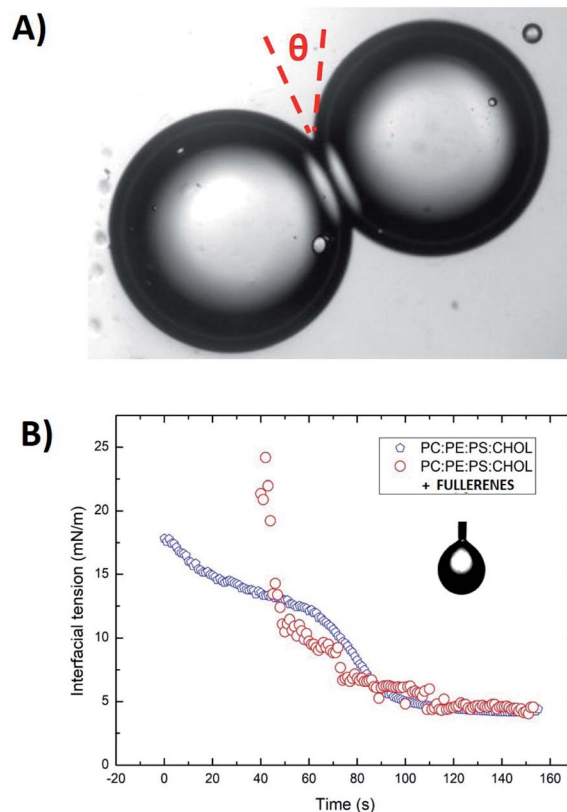

Fig. 1 (A) A DiB formed by two water droplets connected by a DOPC bilayer in squalene, and the associated contact angle θ. (B) Example of interfacial tension measurements of a water/oil–lipid mixture with the water pendant droplet method (blue square). The oil is squalene with a mixture of dissolved lipids ($c \approx 5$ mg mL^{-1}), DOPC : DOPS : DOPE with 70 : 10 : 20 molar ratio and 40% cholesterol. In a second trace, plotted with red circles, is the same oil and lipid composition with 40 μg mL^{-1} of fullerenes.

a dichroic mirror, a laser cut-off filter and an excitation filter (LaVision). The fluorescent sample can be excited through the same objective used for image recording by a green laser ($\lambda =$ 532 nm, pulsed DPSS, 2.72 W, LaVision), coupled to the microscope by a multi-mode glass fiber. The fluorescence signal emitted by the sample is isolated from scattered laser light by the filter cube assembly and recorded by a camera (Imager Pro X, Lavision) coupled with the microscope by a camera adapter (Zeiss).

2.5 Water permeability analysis

When two osmotically imbalanced droplets are separated by a lipid bilayer, water transport immediately started between these two droplets. Changes in droplet size due to this water transport were thus measured from the commencement of this process. Fig. 2A shows an example of such a system, where the leftmost droplet in the images contains NaCl (100 mM) with an accurately known osmolality in the range of 200 m Osm kg^{-1}. The osmotic gradient drives water transport through the droplet bilayer. This resulted in a change in droplet diameter as a function of time Fig. 2. The total volume change of the growing droplet is measured automatically as a function of time t, *via* commercial image analysis software (Image-ProPlus from MediaCybernetics). This volume change allowed us to determine water transport through the bilayer contact area A, which

is then used to determine the water permeability coefficient P_f. Indeed, the analyzed volume variation as a function of time, dV/dt, can be expressed by the following equation:[19–23]

$$\frac{dV(t)}{dt} = -P_f A(t) v_w \Delta C(t) \tag{2}$$

where A is the bilayer area, v_w is the molar volume of water (18 mL mol^{-1}), $\Delta C(t)$ is the time-dependent osmolarity gradient between the two droplets, and P_f is the bilayer permeability coefficient of water. As the bilayer contact area $A(t)$ is constant, the time evolution of the swelling droplet can be obtained from the integration of eqn (2), since the shrinking droplet contains no osmolyte, its concentration could be considered as constant and thus we obtain:[19–24]

$$\left(\frac{V}{V_0}\right)^2 = 1 + \left(\frac{2P_f A v_w C_0}{V_0}\right)t \tag{3}$$

An example of such analysis is plotted (Fig. 2D), where the volume change, $\left(\frac{V}{V_0}\right)^2$, appears to be proportional to time, t, as predicted by eqn (3). Please note that this analysis is only possible when the bilayer area A stays constant, which is the case only for a short time after bilayer formation. Indeed, due to the high bilayer tension, the bilayer area sometimes has the tendency to expand strongly after ≈ 5–10 min.
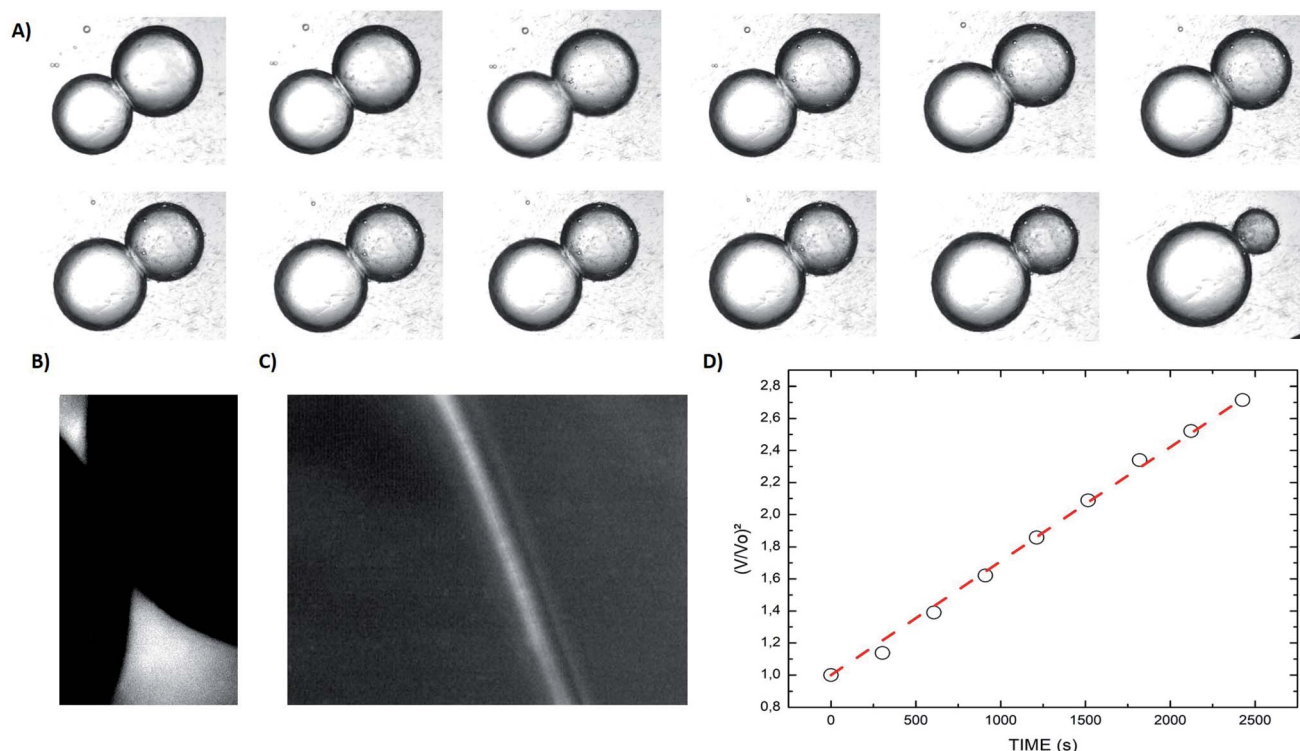

Fig. 2 (A) Time series of a DiB formed by 2 water droplets connected by a bilayer made of DOPC : DOPS : DOPE with 70 : 10 : 20 molar ratio and 40% cholesterol. The left droplet contains 100 mM of NaCl. At the start, the right droplet has a diameter equal to 0.6 mm. The timeframe between each picture is 303 s. The left droplet contains 100 mM of NaCl. (B) Fluorescent picture of a DiB, the fluorescent molecule Rho-DOPE is only visible in the oil phase. 40 μg mL^{-1} of fullerene are also dissolved into the oily phase. No fluorescent molecules are visible in the droplets. (C) Image of the fluorescent bilayer observed with higher magnification. (D) Droplet shape analysis from the pictures in (A).

3 Results and discussion

3.1 Water permeability of a physiological lipid bilayer as a function of the concentration of cholesterol and fullerene

Water permeability of a model cell membrane has been extensively studied in the last few decades. These studies present huge differences depending on the choice of molecules the lipid bilayer comprises of, but also with the type of experimental setup employed to perform these measurements. For example, water permeability measurements performed with the DiB technique reported permeability coefficient $P_f \approx 50\text{--}100~\mu m~s^{-1}$ for a bilayer made with single chain lipids (monoglyceride),[22] or with archaeal lipids (DPhPC).[23] These permeability coefficients are massively slower than the permeability coefficients $P_f \approx 1\text{--}0.01~cm~s^{-1}$ measured with a DiB made of PC (phosphatidylcholine) lipids.[19] These differences highlight the importance of the lipidic molecules that comprise the considered lipid bilayer. However, notable differences are also reported for different model systems with similar lipidic compositions. As an example, water permeability coefficients obtained from vesicles made of PC lipids are different from measurements with a DiB system while having identical lipidic compositions.[19,25,26] These difference could be explained by several factors, one is that the bilayer geometry and, therefore, the lipid bending and packing is changing between a planar or a spherical bilayer.[27] This effect even depends on the vesicle size, as confirmed experimentally by measuring different permeability coefficients for different vesicle sizes of identical lipidic composition.[25,26] Another point is that the bilayer tension changes with the method of formation of the lipid bilayer, in particular the DiB technique produces a bilayer with a relatively high tension (1–12 mN m^{-1})[18,28] in comparison to the tension of native lipid vesicles (0.01–1 mN m^{-1}).[29] Considering these facts, from herein, we only compare my results with those reported with the same model system, *i.e.*, the DiB technique. However, even systems produced by the DiB technique may present large differences. In particular, a solvent is often added to oil–lipid mixtures in order to reduce the bilayer tension and thus increase the stability of the bilayer.[17] In this article, we only produce DiB without solvents and with an oil–lipid composition that does not affect the physiological relevance of this lipid bilayer. As the oil, we choose to use squalene oil, as its allow the formation of an oil-free lipid bilayer.[30] We consider than a lipid bilayer with a physiologically relevant composition is made of a mixture of PC (phosphatidylcholine), PE (phosphatidylethanolamine), PS (phosphatidylserine) and cholesterol, as they are the main lipidic components of human cell membranes.[30,31]

We investigate the water permeability across a bilayer with only DOPC lipids, by forming a DiB with a first droplet that contains 100 mM (NaCl) and a second droplet that contains no salt. The measured water permeability of $P_f \approx 0.4~cm~s^{-1}$ is similar to values calculated from numerical simulations made with a planar DOPC bilayer.[32] Adding 10% DOPS in a molar ratio to the bilayer composition, no notable change of the water permeability coefficient across the bilayer was measured (in agreement with ref. 33). However, after adding 20% DOPE in

a molar ratio, a decrease of the water permeability $P_f \approx 0.2~cm~s^{-1}$ across the bilayer was found. This reduction could be understood as PE lipids have a higher chain order than PC lipids.[25,34] The order increase from the addition of PE instead of PC, gave higher lipid packing density and a smaller area per molecule,[25,35] which reduces the water permeability of the bilayer. Another reason is that the bilayer tension is reduced by the addition of DOPE (from ≈ 8 to $\approx 4~mN~m^{-1}$), which reduces the bilayer thickness and therefore its water permeability.[36] It results that the measured permeability of the DOPC : DOPE : DOPS bilayer (70 : 20 : 10 in molar ratio) $P_f \approx 0.2~cm~s^{-1}$ is similar to values calculated for DOPC : DOPE lipid bilayers,[32] which seems to indicate that PS lipids do not affect the permeability of the formed bilayer significantly. Then, we increase the concentration of cholesterol in the bilayer composition to 20% and 40% total molar ratio. The corresponding measurements show a decrease of the water permeability from $\approx 0.15~cm~s^{-1}$ to $\approx 0.08~cm~s^{-1}$, respectively. These measurements are in agreement with the literature.[37] It is supposed that cholesterol reduces the bilayer water permeability because it is known to increase the thickness of this bilayer.[36–38] These results also confirm that the formed bilayer is really an oil-free bilayer.[17,30] The energetics of water permeation could be extracted *via* an Arrhenius plot,[20–23] by plotting $\ln(P_f)$ *versus* $1/T$, where T is the temperature in Kelvin (see Fig. 3). This curve appears to be linear, where the slope of this curve is equal to E_a/R, where E_a is the activation energy and R is the gas constant.[20–23] The extracted activation energies are in the typical range of the previous values reported in the literature (see Fig. 3 and Table 1).[20–23,25,32]

Now that we have described the water permeability of a physiological lipid bilayer formed by the DiB technique. We can shed some light on the water permeability across a lipid bilayer doped with fullerenes. Adding a low concentration $c \approx 10~\mu g~mL^{-1}$ of fullerenes to the oil, enhances the water permeability across the formed lipid bilayer (see Fig. 3). This measured water permeability increases with the concentration of fullerenes dissolved into the oily phase, up to a concentration of $\approx 40~\mu g~mL^{-1}$. This effect could be seen as a surprise, because hydrophobic nanoparticles, or polymers, are supposed to accumulate in the bilayer core. Thus, this agglomerate of nano-objects increases the thickness of the bilayer and should decreases the bilayer permeability.[36,39] Conversely, we measured an increase of the water permeability as a function of the fullerene concentration. A second surprise, this increases of permeability seems to be independent of the bilayer fluidity. Indeed, the bilayer adhesion energy ΔF that tunes the fluidity of the drop pair can be expressed from eqn(1), see eqn (4)

$$\Delta F = 2\gamma(1 - \cos(\theta)). \tag{4}$$

The result is that the bilayer tension and the bilayer fluidity are nearly constant with and without fullerene, for the tested lipid composition PC : PS : PE (70 : 10 : 20) and 40% cholesterol (Fig. 1A and B). A similar effect of enhanced water permeability as a function of the concentration of fullerenes, was also observed in the numerical simulation by Su *et al.*[16,40] In their
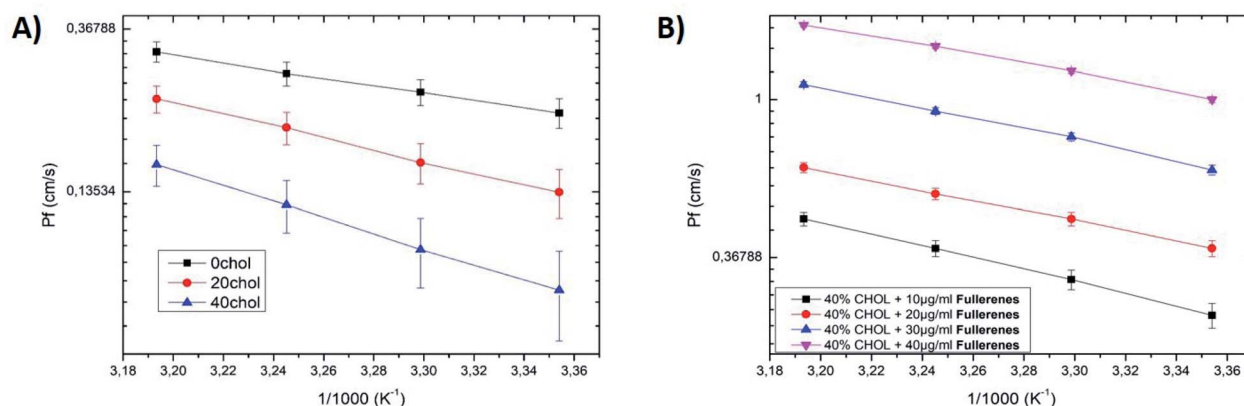
Fig. 3 (A) Arrhenius plot of the natural log of the permeability coefficient (P_f) versus the reciprocal of absolute temperature of membranes of DOPC : DOPS : DOPE (70 : 10 : 20 molar ratio) membranes, with different cholesterol concentrations: 0%, 20%, 40%. (B) Arrhenius plot of the natural log of the permeability coefficient (P_f) versus the reciprocal of absolute temperature of DOPC : DOPS : DOPE (70 : 10 : 20 molar ratio) membranes, with 40% cholesterol and doped with fullerenes at different concentrations.

studies, they report an increase of the water permeability across a lipid bilayer as a function of ultra-small nanoparticles depending of their hydrophobicity.[16,40] They justify this surprising effect by the measured increase in the area per lipid due to the interaction between the hydrophobic nanoparticles and the lipid bilayer molecules.[16] Even if they did not consider exactly the case of fullerenes, their nanoparticles are comparable in term of size and hydrophobicity. Nevertheless, it is difficult to make a quantitative comparison between this study and such theoretical work. As we ignore the real fullerenes concentration (cluster) inside the lipid bilayer and we do not know the precise hydrophobicity of the tested fullerenes. To explore more deeply the fullerenes interaction with the lipid bilayer, we produced some capacitance experiments with a freestanding bilayer in a μ-chip following the method described by Guo et al.[41] This microfluidic method and results are fully described in the ESI.† With this microfluidic platform, we measured the thickness of this freestanding bilayer using capacitance measurements. It results that the bilayer thickness increases as a function of the fullerenes concentration, while the water permeability decreases as a function of the fullerenes concentration (with the DiB technique). To demonstrate the

specificity of fullerenes, we repeated these capacitance measurements with gold hydrophobic nanoparticles of similar diameter (≈1 nm) embedded into a freestanding lipid bilayer. This demonstrates that these gold nanoparticles increase the bilayer thickness, like fullerene, but reduce the permeability of the bilayer (ESI†). As gold nanoparticles and fullerene are both extremely hydrophobic, they could be considered as similar in terms of hydrophobicity and size. The only difference between them is that gold nanoparticles are not electrically conducting, while fullerenes are electrically conducting. Therefore, we might propose that the conducting properties of the fullerenes play a key role in the enhanced water permeability of the lipid bilayer. After increasing the concentration of fullerene above $c \approx 40$ μg mL^{-1} no stable lipid bilayer could be formed via the DiB technique. The corresponding lipid bilayer breaks shortly after its formation. This rupture suggests the presence of large fullerene clusters inside the lipid bilayer as a reason for its instability.[41] This hypothesis is supported by the fact that some fullerene clusters with microscopic size are already visible in the oily phase using bright field microscopy. Moreover the fullerenes are known to have dissolution issues.[10] A natural question is: what if these fullerene clusters may create some pores or even

Table 1 Summary of the activation energies (E_a) and water permeability coefficients (P_f) as a function of the temperature (in Kelvin) and bilayer composition

Bilayer composition (PC : PS : PE)	P_f at 298.15 K	P_f at 303.15 K	P_f at 308.15 K	P_f at 313.15 K	E_a
70 : 10 : 20	0.22 cm s^{-1}	0.25 cm s^{-1}	0.28 cm s^{-1}	0.32 cm s^{-1}	4.5 (kcal mol^{-1})
70 : 10 : 20 + 20% CHOL	0.135 cm s^{-1}	0.162 cm s^{-1}	0.201 cm s^{-1}	0.24 cm s^{-1}	7.1 (kcal mol^{-1})
70 : 10 : 20 + 40% CHOL	0.074 cm s^{-1}	0.095 cm s^{-1}	0.125 cm s^{-1}	0.16 cm s^{-1}	9.5 (kcal mol^{-1})
70 : 10 : 20 + 40% CHOL + 10 μg mL^{-1} fullerenes	0.25 cm s^{-1}	0.32 cm s^{-1}	0.39 cm s^{-1}	0.47 cm s^{-1}	7.5 (kcal mol^{-1})
70 : 10 : 20 + 40% CHOL + 20 μg mL^{-1} fullerenes	0.39 cm s^{-1}	0.47 cm s^{-1}	0.55 cm s^{-1}	0.65 cm s^{-1}	6.2 (kcal mol^{-1})
70 : 10 : 20 + 40% CHOL + 30 μg mL^{-1} fullerenes	0.64 cm s^{-1}	0.79 cm s^{-1}	0.93 cm s^{-1}	1.1 cm s^{-1}	6.6 (kcal mol^{-1})
70 : 10 : 20 + 40% CHOL + 40 μg mL^{-1} fullerenes	1 cm s^{-1}	1.2 cm s^{-1}	1.4 cm s^{-1}	1.6 cm s^{-1}	5.8 (kcal mol^{-1})

translocate spontaneously outside the bilayer using a lipid-wrapping process?[41] We tested these possibilities by observing a lipid bilayer made of fluorescent lipids, and it appears that no visible lipid extraction could be measured. Electrophysiological inspection has also been performed on the formed bilayer, following the method reported by Guo *et al.*[41] and no nanopores could be measured. Therefore, it could be safely assumed that the fullerenes embedded into the bilayer core do not generate pores, or escape from this bilayer. Considering the activation energies, the Arrhenius plots (Fig. 3) show some notable differences with the activation energies measured for a bilayer without fullerenes. This indicates a change in the enthalpy of activation ΔH of the lipid bilayer when it is doped with fullerenes, as $E_a = \Delta H + RT$.[42] Moreover, we measured a clear reduction of the activation energies as a function of the concentration of fullerenes.

Additionally, this study was performed with C60 fullerenes. We tried to reproduce this work with C70 fullerenes, but no stable bilayer could be formed for the tested fullerene concentration. In particular no *zipping* could be observed, which suggests a very strong interaction between the C70 fullerenes and the lipid molecules.

4 Conclusions

We produce a lipid bilayer by the DiB technique, which consists of bringing into contact two water droplets in a lipid–oil mixture. An osmotic pressure gradient is create by tuning the salt concentration between these two droplets. Then, the water permeability coefficient of this bilayer is obtained by measuring the droplet volume change generate by the water transfer across this bilayer. The measured water permeability coefficients are reported as a function of cholesterol concentration. The measured water permeability coefficients decrease with increasing cholesterol concentration, as reported in the literature. And, consistently, the associated activation energies increase with the cholesterol concentration. Then, we extend this study by doping the bilayers with fullerenes. It appears that fullerenes enhance the water permeability across a lipid bilayer. This effect could be seen as a surprise, because fullerenes accumulate into the bilayer core which increases the thickness of the bilayer and therefore should decrease the permeability of the bilayer. In contrast of such expectations, we observed a significant increase of the bilayer permeability as a function of the concentration of fullerenes. After comparing with hydrophobic gold nanoparticles of the same size, it appears that they accumulate in the bilayer core and increase the thickness of the bilayer. But opposite to the effect of fullerenes, the gold nanoparticles showed a decrease of the bilayer permeability. The only difference between these two types of nanoparticles is that gold nanoparticles are not electrically conducting, while fullerenes are electrically conducting. Therefore, it can be proposed that the conducting properties of the fullerenes might play a key role in the enhanced water permeability of the lipid bilayer. This enhanced permeability appears to be independent of the bilayer fluidity, which is in contrast to the typical behavior of other model systems. This confirms the possibility of a new

physical process behind this enhanced permeability. Above a maximum concentration of fullerene, the formed bilayer becomes unstable. The bilayer rupture may be due to the presence of fullerene clusters. This study highlights a possible role of fullerene as a drug to enhance water permeability in the case of cells that present abnormal water transport properties. This study may also be useful in the design of new filtering processes. It raises questions about the influence of other types of ultra-small hydrophobic objects on the transport properties of cell membranes.

Conflicts of interest

There are no conflicts to declare.

Acknowledgements

References

1 E. Castro, A. H. Garcia, G. Zavala and L. Echegoyen, *J. Mater. Chem. B*, 2017, **5**, 6523–6535.

2 S. H. Friedman, D. L. DeCamp, R. P. Sijbesma, G. Srdanov, F. Wudl and G. L. Kenyon, *J. Am. Chem. Soc.*, 1993, **115**, 6506–6509.

3 V. A. Chistyakov, Y. O. Smirnova, E. V. Prazdnova and A. V. Soldatov, *BioMed Res. Int.*, 2013, **2013**, 1–4.

4 R. D. Bolskar, in *Encyclopedia of Nanotechnology*, ed. B. Bhushan, Springer Netherlands, Dordrecht, 2016, pp. 1267–1281.

5 D. Mi, J.-H. Kim, H. U. Kim, F. Xu and D.-H. Hwang, *J. Nanosci. Nanotechnol.*, 2014, **14**, 1064–1084.

6 P. A. Troshin, H. Hoppe, J. Renz, M. Egginger, J. Y. Mayorova, A. E. Goryachev, A. S. Peregudov, R. N. Lyubovskaya, G. Gobsch, N. S. Sariciftci and V. F. Razumov, *Adv. Funct. Mater.*, 2009, **19**, 779–788.

7 H. Jung, C.-U. Wang and W. Jang, *J. Toxicol. Environ. Health Sci.*, 2009, **1**, 132–139.

8 G. Andrievsky, V. Klochkov and L. Derevyanchenko, *Fullerenes, Nanotubes, Carbon Nanostruct.*, 2005, **13**, 363–376.

9 J. Kolosnjaj, H. Szwarc and F. Moussa, in *Bio-Applications of Nanoparticles*, ed. N. Back, I. R. Cohen, A. Lajtha, J. D. Lambris, R. Paoletti and W. C. W. Chan, Springer New York, New York, NY, 2007, vol. 620, pp. 168–180.

10 R. S. Ruoff, D. S. Tse, R. Malhotra and D. C. Lorents, *J. Phys. Chem.*, 1993, **97**, 3379–3383.

11 J. Barnoud, G. Rossi and L. Monticelli, *Phys. Rev. Lett.*, 2014, **112**, 068102.

12 J. Zupanc, D. Drobne, B. Drasler, J. Valant, A. Iglic, V. Kralj-Iglic, D. Makovec, M. Rappolt, B. Sartori and K. Kogej, *Carbon*, 2012, **50**, 1170–1178.

13 A. Ikeda, M. Mori, K. Kiguchi, K. Yasuhara, J.-i. Kikuchi, K. Nobusawa, M. Akiyama, M. Hashizume, T. Ogawa and T. Takeya, *Chem.–Asian J.*, 2012, **7**, 605–613.

14 W. Stillwell, *An Introduction to Biological Membranes Composition, Structure and Function Book*, 2nd edn, 2016,

ISBN 978-0-444-63772-7, https://www.sciencedirect.com/book/9780444637727/an-introduction-to-biological-membranes.

15 J. Brahm, *J. Exp. Biol.*, 2013, **216**, 2238–2246.

16 C.-F. Su, H. Merlitz, H. Rabbel and J.-U. Sommer, *J. Phys. Chem. Lett.*, 2017, **8**, 4069–4076.

17 H. Bayley, B. Cronin, A. Heron, M. A. Holden, W. L. Hwang, R. Syeda, J. Thompson and M. Wallace, *Mol. BioSyst.*, 2008, **4**, 1191.

18 J. Bibette, F. L. Calderon and P. Poulin, *Rep. Prog. Phys.*, 1999, **62**, 969–1033.

19 A. R. Thiam, N. Bremond and J. Bibette, *Langmuir*, 2012, **28**, 6291–6298.

20 M. Lopez, S. E. Evangelista, M. Morales and S. Lee, *Langmuir*, 2017, **33**, 900–912.

21 M. Lopez, J. Denver, S. E. Evangelista, A. Armetta, G. Di Domizio and S. Lee, *Langmuir*, 2018, **34**, 2147–2157.

22 Z. Michalak, M. Muzzio, P. J. Milianta, R. Giacomini and S. Lee, *Langmuir*, 2013, **29**, 15919–15925.

23 P. J. Milianta, M. Muzzio, J. Denver, G. Cawley and S. Lee, *Langmuir*, 2015, **31**, 12187–12196.

24 S. S. Dixit, A. Pincus, B. Guo and G. W. Faris, *Langmuir*, 2012, **28**, 7442–7451.

25 D. Huster, A. Jin, K. Arnold and K. Gawrisch, *Biophys. J.*, 1997, **73**, 855–864.

26 M. Jansen and A. Blume, *Biophys. J.*, 1995, **68**, 997–1008.

27 W.-j. Tien, K.-y. Chen, F.-y. Huang and C.-c. Chiu, *Int. J. Mater. Sci.*, 2019, **20**, 3252.

28 Y. Guo, M. Werner, R. Seemann, V. A. Baulin and J.-B. Fleury, *ACS Nano*, 2018, **12**, 12042–12049.

29 R. Dimova, *Annu. Rev. Biophys.*, 2019, **48**, 93–119.

30 P. Heo, S. Ramakrishnan, J. Coleman, J. E. Rothman, J. Fleury and F. Pincet, *Small*, 2019, **15**, 1900725.

31 G. van Meer, D. R. Voelker and G. W. Feigenson, *Nat. Rev. Mol. Cell Biol.*, 2008, **9**, 112–124.

32 M. Palaiokostas, W. Ding, G. Shahane and M. Orsi, *Soft Matter*, 2018, **14**, 8496–8508.

33 W. Shinoda, *Biochim. Biophys. Acta, Biomembr.*, 2016, **1858**, 2254–2265.

34 M. Lafleur, B. Fine, E. Sternin, P. R. Cullis and M. Bloom, *Biophys. J.*, 1989, **56**, 1037–1041.

35 F. Separovic and K. Gawrisch, *Biophys. J.*, 1996, **71**, 274–282.

36 J. F. Nagle, J. C. Mathai, M. L. Zeidel and S. Tristram-Nagle, *J. Gen. Physiol.*, 2007, **131**, 77–85.

37 J. C. Mathai, S. Tristram-Nagle, J. F. Nagle and M. L. Zeidel, *J. Gen. Physiol.*, 2008, **131**, 69–76.

38 Y. Guo, M. Werner, J. B. Fleury and V. A. Baulin, *Phys. Rev. Lett.*, 2020, **124**, 038001.

39 D. Bochicchio, E. Panizon, L. Monticelli and G. Rossi, *Sci. Rep.*, 2017, **7**, 6357.

40 C.-F. Su, H. Merlitz, F. Thalmann, C. Marques and J.-U. Sommer, *J. Phys. Chem. C*, 2019, **123**, 6839–6848.

41 Y. Guo, E. Terazzi, R. Seemann, J. B. Fleury and V. A. Baulin, *Sci. Adv.*, 2016, **2**, e1600261.

42 M. Sogami, S. Era, M. Murakami, Y. Seo, H. Watari and N. Uyesaka, *Biochim. Biophys. Acta, Biomembr.*, 2001, **1511**, 42–48.